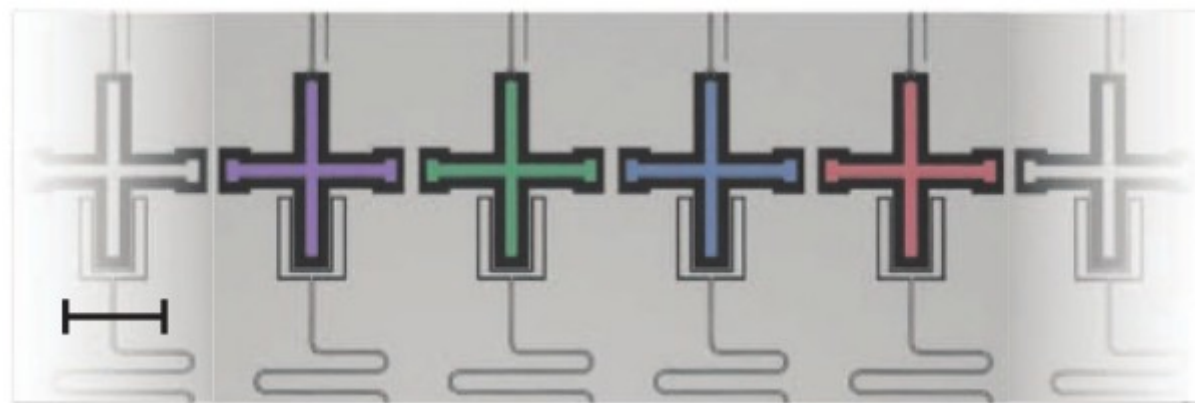
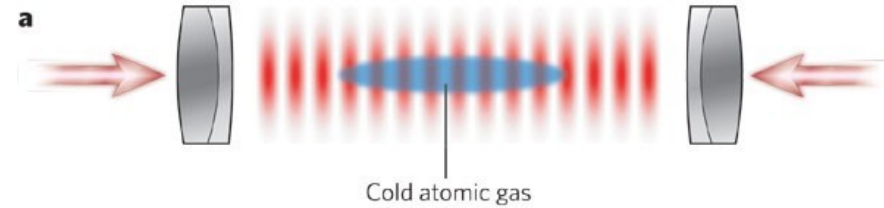


Digital quantum simulation of fermionic models with a superconducting circuit

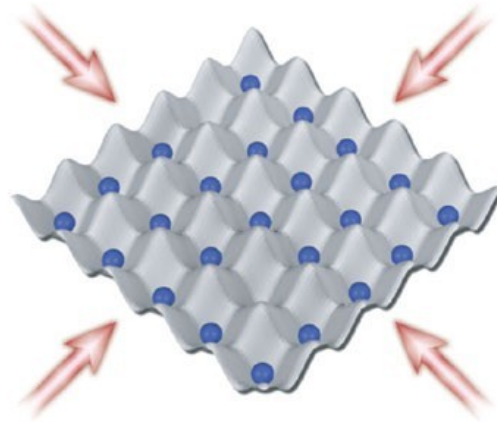
R. Barends¹, L. Lamata², J. Kelly^{3,†}, L. García-Álvarez², A.G. Fowler¹, A. Megrant^{3,4}, E. Jeffrey¹, T.C. White³, D. Sank¹, J.Y. Mutus¹, B. Campbell³, Yu Chen¹, Z. Chen³, B. Chiaro³, A. Dunsworth³, I.-C. Hoi³, C. Neill³, P.J.J. O'Malley³, C. Quintana³, P. Roushan¹, A. Vainsencher³, J. Wenner³, E. Solano^{2,5} & John M. Martinis^{1,3}



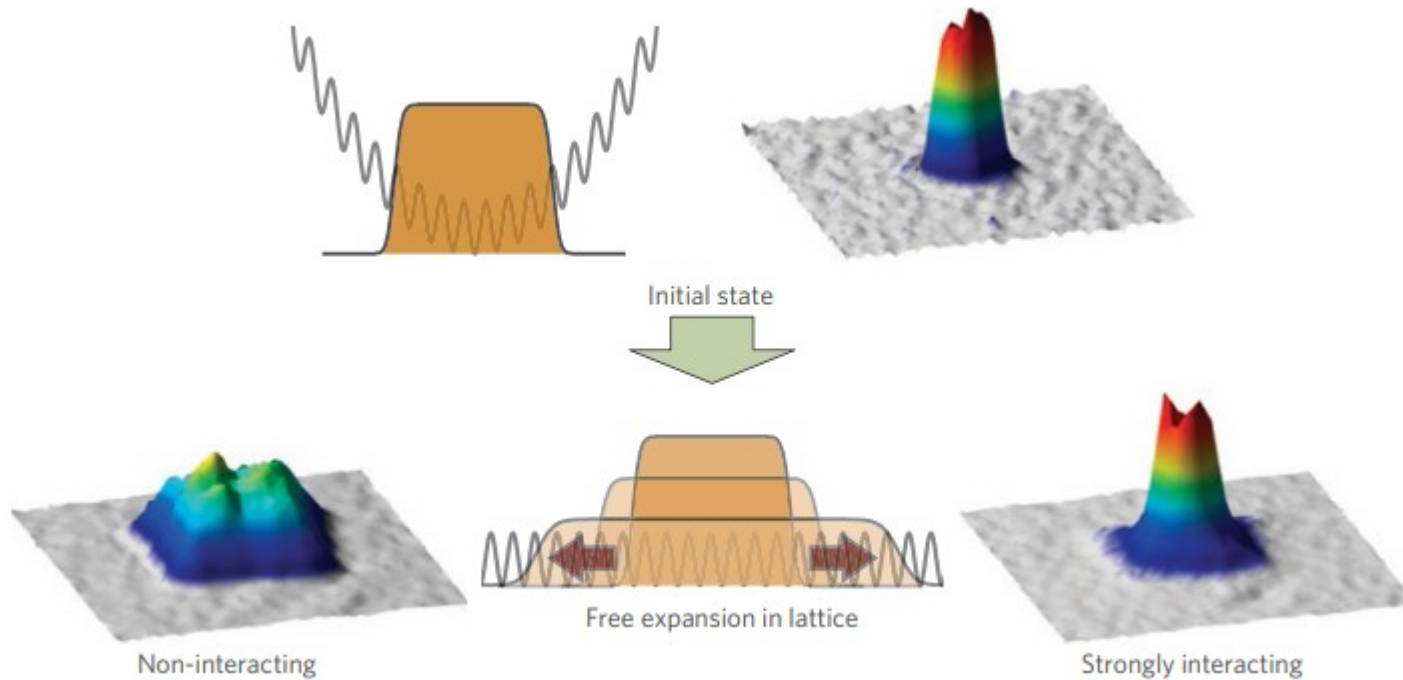
Analog quantum computation



b

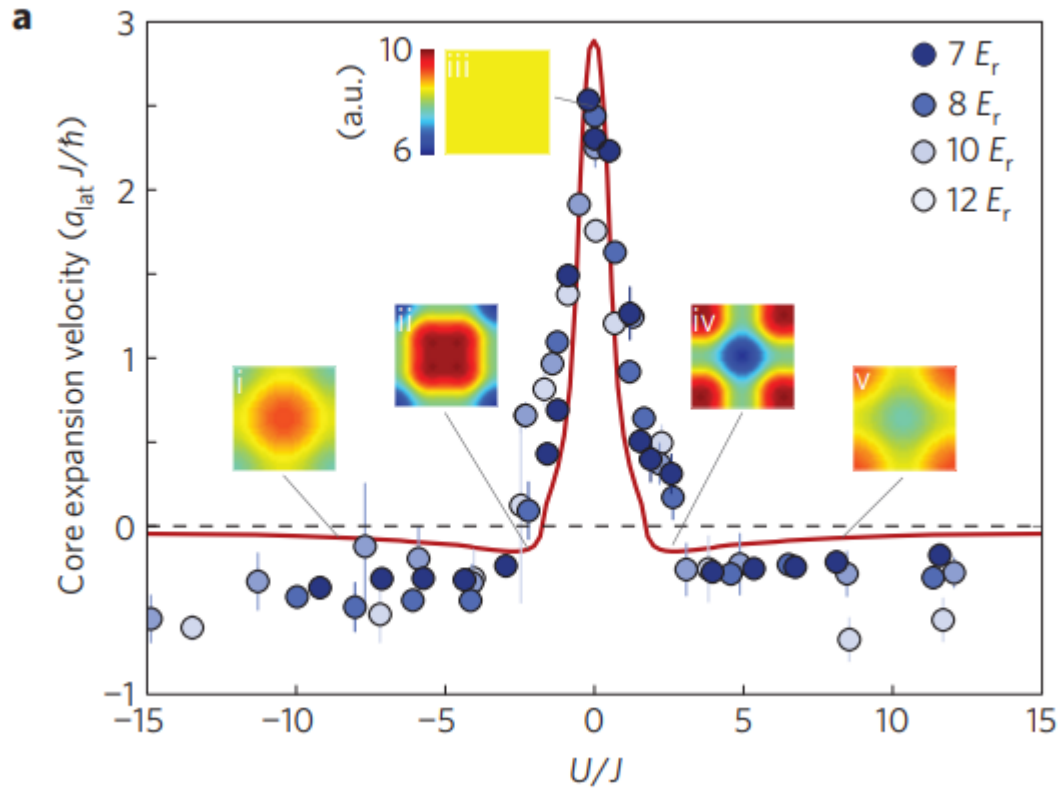


Analog quantum computation

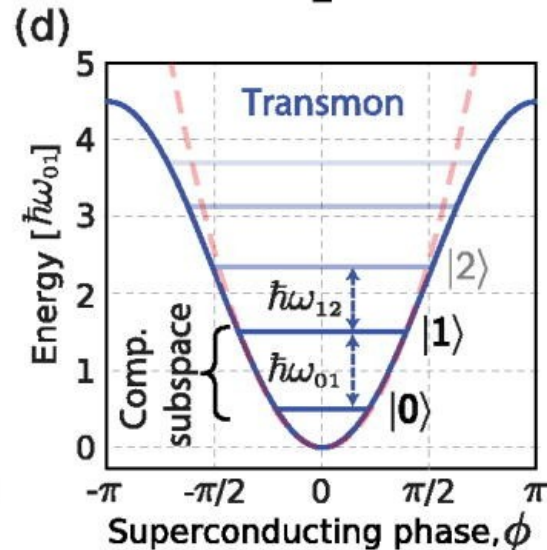
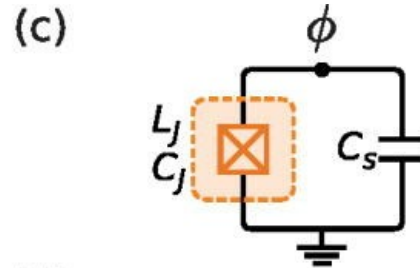
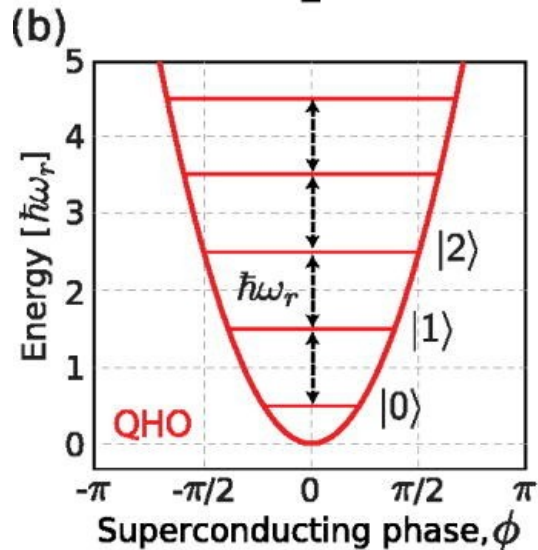
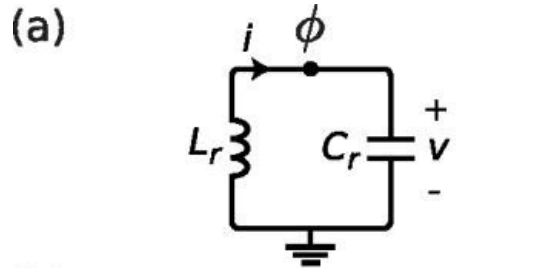


Schneider, U., Hackermüller, L., Ronzheimer, J. et al. Fermionic transport and out-of-equilibrium dynamics in a homogeneous Hubbard model with ultracold atoms. *Nature Phys* 8, 213 (2012).

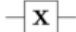

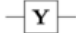
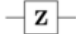
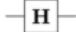

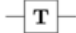

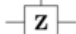
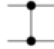

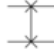
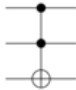
Analog quantum computation



Digital quantum computation



Quantum gates

Operator	Gate(s)	Matrix
Pauli-X (X)	 	$\begin{bmatrix} 0 & 1 \\ 1 & 0 \end{bmatrix}$
Pauli-Y (Y)		$\begin{bmatrix} 0 & -i \\ i & 0 \end{bmatrix}$
Pauli-Z (Z)		$\begin{bmatrix} 1 & 0 \\ 0 & -1 \end{bmatrix}$
Hadamard (H)		$\frac{1}{\sqrt{2}} \begin{bmatrix} 1 & 1 \\ 1 & -1 \end{bmatrix}$
Phase (S, P)		$\begin{bmatrix} 1 & 0 \\ 0 & i \end{bmatrix}$
$\pi/8$ (T)		$\begin{bmatrix} 1 & 0 \\ 0 & e^{i\pi/4} \end{bmatrix}$
Controlled Not (CNOT, CX)		$\begin{bmatrix} 1 & 0 & 0 & 0 \\ 0 & 1 & 0 & 0 \\ 0 & 0 & 0 & 1 \\ 0 & 0 & 1 & 0 \end{bmatrix}$
Controlled Z (CZ)	 	$\begin{bmatrix} 1 & 0 & 0 & 0 \\ 0 & 1 & 0 & 0 \\ 0 & 0 & 1 & 0 \\ 0 & 0 & 0 & -1 \end{bmatrix}$
SWAP	 	$\begin{bmatrix} 1 & 0 & 0 & 0 \\ 0 & 0 & 1 & 0 \\ 0 & 1 & 0 & 0 \\ 0 & 0 & 0 & 1 \end{bmatrix}$
Toffoli (CCNOT, CCX, TOFF)		$\begin{bmatrix} 1 & 0 & 0 & 0 & 0 & 0 & 0 & 0 \\ 0 & 1 & 0 & 0 & 0 & 0 & 0 & 0 \\ 0 & 0 & 1 & 0 & 0 & 0 & 0 & 0 \\ 0 & 0 & 0 & 1 & 0 & 0 & 0 & 0 \\ 0 & 0 & 0 & 0 & 1 & 0 & 0 & 0 \\ 0 & 0 & 0 & 0 & 0 & 1 & 0 & 0 \\ 0 & 0 & 0 & 0 & 0 & 0 & 0 & 1 \\ 0 & 0 & 0 & 0 & 0 & 0 & 1 & 0 \end{bmatrix}$

Simulating interacting fermions

Hubbard model:

$$H = -V \sum_{\langle i,j \rangle} (b_i^\dagger b_j + b_j^\dagger b_i) + U \sum_{i=1}^N n_{i\uparrow} n_{i\downarrow}$$

insightful to look at a fermionic two-mode example,

$$H = -V (b_1^\dagger b_2 + b_2^\dagger b_1) + U b_1^\dagger b_1 b_2^\dagger b_2.$$

$$\left. \begin{aligned} S_j^z &= f_j^\dagger f_j - \frac{1}{2}, \\ S_j^+ &= f_j^\dagger e^{i\pi \sum_{l<j} n_l}, \\ S_j^- &= f_j e^{-i\pi \sum_{l<j} n_l} \end{aligned} \right\} \text{Jordan Wigner transformation}$$

$$\begin{aligned} n_j &\leftrightarrow (\sigma_j^z + 1)/2 \\ c_j &\leftrightarrow (-1)^{\sum_{l<j} n_l} \sigma_j^- \\ c_j^\dagger &\leftrightarrow (-1)^{\sum_{l<j} n_l} \sigma_j^+ \end{aligned}$$

$$b_1^\dagger = I \otimes \sigma^+$$

$$b_2^\dagger = \sigma^+ \otimes \sigma_z$$

$$b_k^\dagger = I_N \otimes I_{N-1} \otimes \cdots \otimes \sigma_k^+ \otimes \sigma_{k-1}^z \otimes \cdots \otimes \sigma_1^z$$

Simulating interacting fermions

$$H = -V \left(b_1^\dagger b_2 + b_2^\dagger b_1 \right) + U b_1^\dagger b_1 b_2^\dagger b_2.$$

$$b_1^\dagger = I \otimes \sigma^+$$

$$b_2^\dagger = \sigma^+ \otimes \sigma_z$$



$$H = \frac{V}{2} \left(\sigma_x \otimes \sigma_x + \sigma_y \otimes \sigma_y \right) + \frac{U}{4} \left(\sigma_z \otimes \sigma_z + I \otimes \sigma_z + \sigma_z \otimes I \right),$$

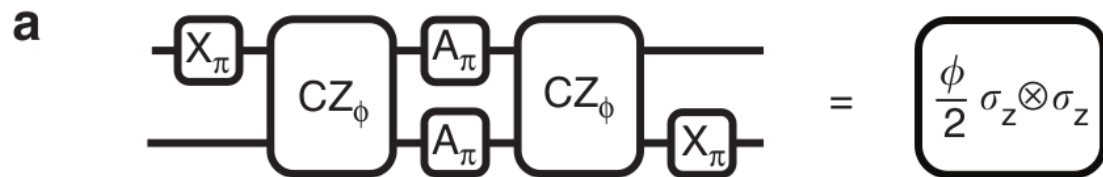
$$\sigma^x \otimes \sigma^x = R_y(\pi/2) \sigma^z \otimes \sigma^z R_y(-\pi/2),$$

$$\sigma^y \otimes \sigma^y = R_x(-\pi/2) \sigma^z \otimes \sigma^z R_x(\pi/2),$$

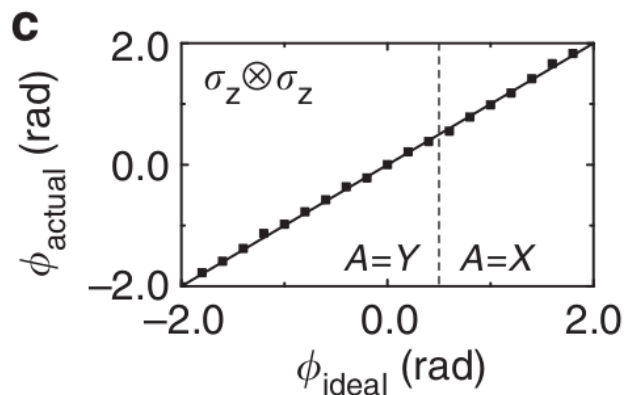
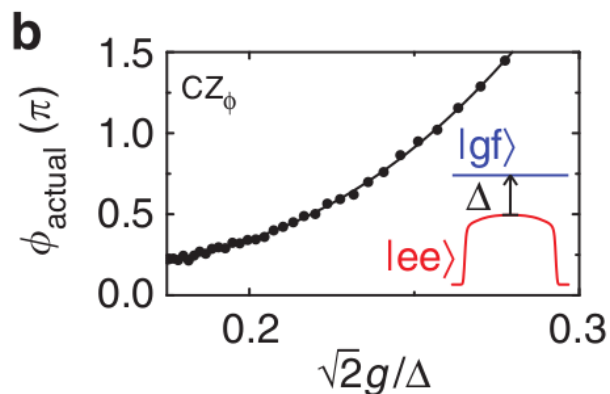
Implementing interactions

$$\exp\left(-i\frac{\phi}{2}\sigma^z \otimes \sigma^z\right) = \begin{pmatrix} 1 & 0 & 0 & 0 \\ 0 & e^{i\phi} & 0 & 0 \\ 0 & 0 & e^{i\phi} & 0 \\ 0 & 0 & 0 & 1 \end{pmatrix}.$$

$$CZ_{q_0, q_1} = I \otimes |0\rangle\langle 0| + Z \otimes |1\rangle\langle 1| = \begin{pmatrix} 1 & 0 & 0 & 0 \\ 0 & 1 & 0 & 0 \\ 0 & 0 & 1 & 0 \\ 0 & 0 & 0 & -1 \end{pmatrix}$$



$$CZ_\phi = \begin{pmatrix} 1 & 0 & 0 & 0 \\ 0 & 1 & 0 & 0 \\ 0 & 0 & 1 & 0 \\ 0 & 0 & 0 & e^{i\phi} \end{pmatrix}$$



Anticommutation check

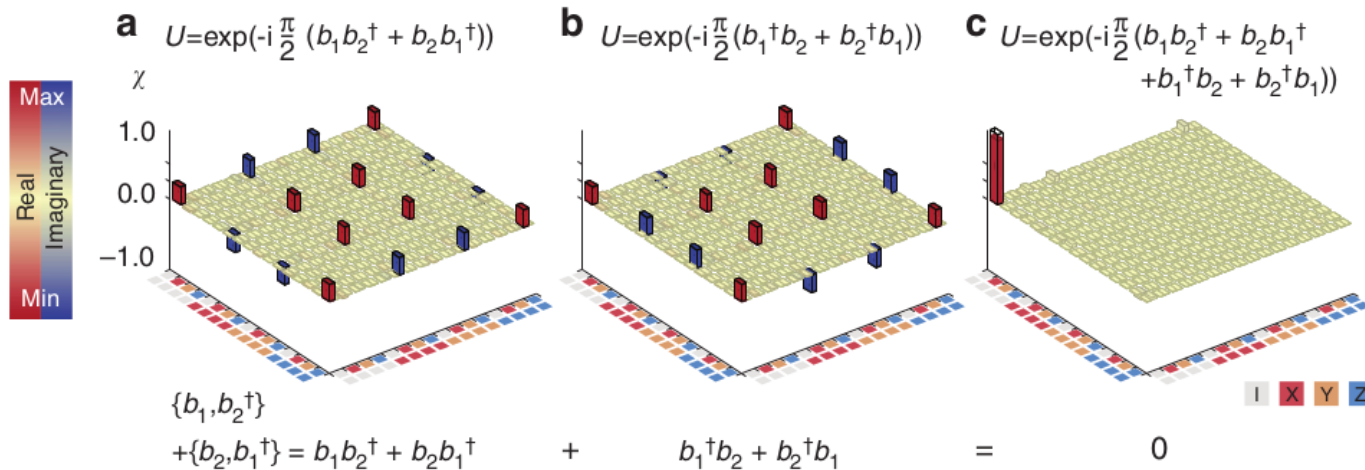


Figure 3 | Quantum process tomography of operator anticommutation. The process matrices are shown for the non-trivial Hermitian terms of the anticommutation relations. **(a)** Process matrix of the unitary $U = \exp(-i\frac{\pi}{2}[b_1b_2^\dagger + b_2b_1^\dagger])$. **(b)** Process matrix of the unitary $U = \exp(-i\frac{\pi}{2}[b_1^\dagger b_2 + b_2^\dagger b_1])$. **(c)** The sequence of both processes, $U = \exp(-i\frac{\pi}{2}[b_1b_2^\dagger + b_2b_1^\dagger + b_1^\dagger b_2 + b_2^\dagger b_1])$, yields the identity. The significant matrix elements, red for the real and blue for the imaginary elements, are close to the ideal (transparent).

Trotter approximation

discuss the simulation of fermionic models. We use the Trotter approximation²⁵ to digitize the evolution of Hamiltonian $H = \sum_k H_k : U = \exp(-iHt) \simeq [\exp(-iH_1 t/n) \exp(-iH_2 t/n) \dots]^n$, with each part implemented using single- and two-qubit gates ($\hbar = 1$). We benchmark the simulation by

Two-mode simulation

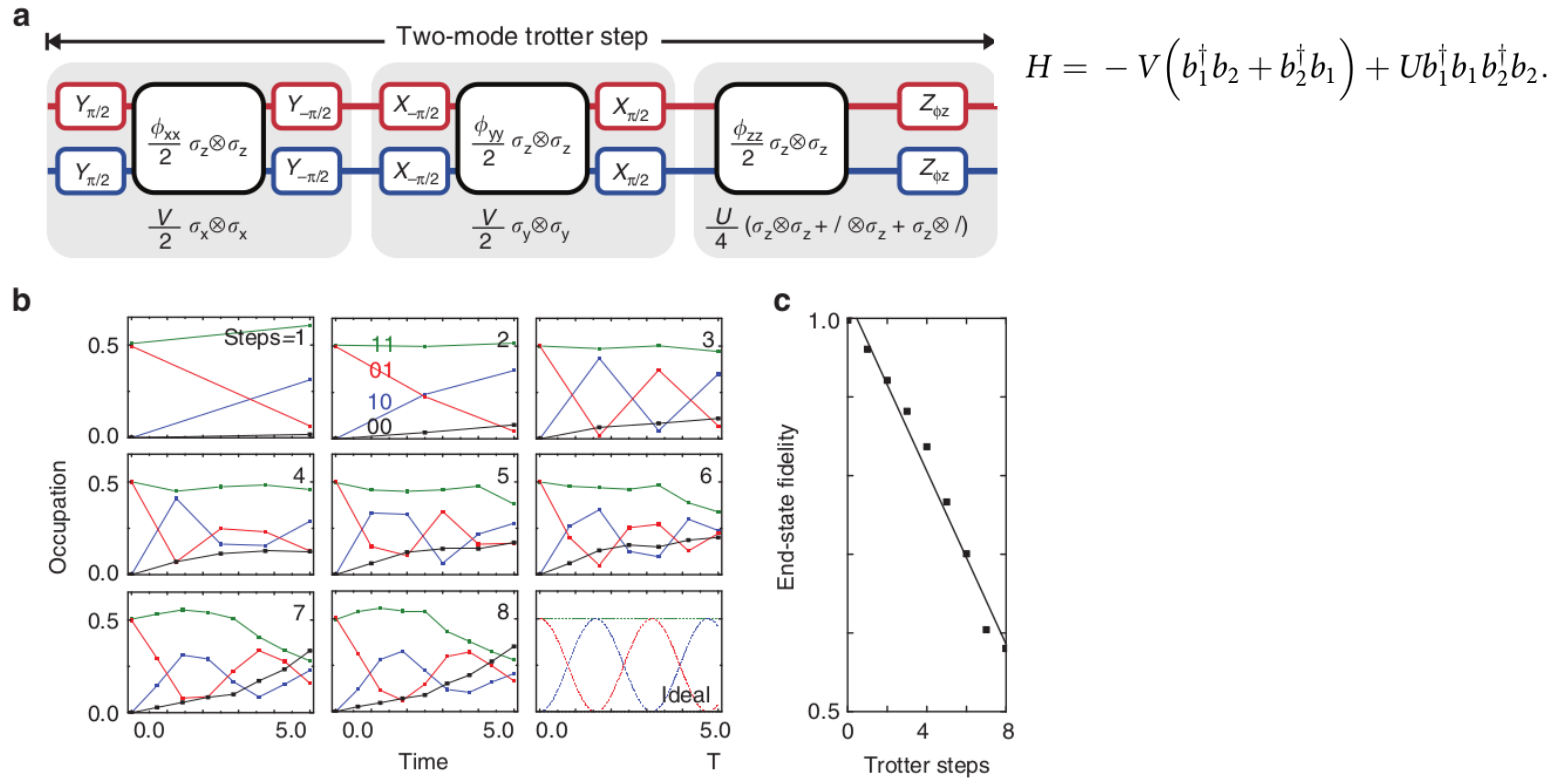


Figure 4 | Simulation of two fermionic modes. (a) Construction of the two-mode Trotter step, showing the separate terms of the Hamiltonian (equation (2)). See Supplementary Note 1 for the pulse sequence and gate count. (b) Occupation of the modes versus simulated time for $n=1, \dots, 8$ steps. Colour coding denotes the state probabilities. Input state is $[(|0\rangle + |1\rangle) \otimes |1\rangle]/\sqrt{2}$, and $V=U=1$. The ideal dependence is shown in the bottom right. The final simulation time is $T=5$. (c) The end-state fidelity decreases with step by 0.054, following a linear trend.

Phase transition

